




Analysis of clinicopathological features and *NAB2-STAT6* fusion variants of meningeal solitary fibrous tumor with ectopic salivary gland components in the cerebellopontine angle

Takahiro Shirakura¹ · Yuichi Yamada² · Satoshi Nakata³ · Bunsho Asayama⁴ · Yoshinobu Seo⁴ · Satoshi Tanikawa^{5,6} · Takayuki Kato⁷ · Nobukazu Komoribayashi^{8,9} · Naohiko Kubo⁹ · Nobuhiro Monma¹⁰ · Naoki Okura¹¹ · Shinya Tanaka^{5,6} · Yoshinao Oda² · Junko Hirato^{1,12} · Hideaki Yokoo¹ · Sumihito Nobusawa¹ 

Received: 17 April 2022 / Revised: 24 August 2022 / Accepted: 25 August 2022 / Published online: 2 September 2022
© The Author(s), under exclusive licence to Springer-Verlag GmbH Germany, part of Springer Nature 2022

Abstract

Solitary fibrous tumors (SFTs) are rare mesenchymal tumors that can occur at any location. Since the identification of specific *NAB2-STAT6* fusion in SFTs, the fusion gene variants, *NAB2* exon 4-*STAT6* exon 2/3 and *NAB2* exon 5/6/7-*STAT6* exon 16/17/18, have been reported to be associated with clinicopathological features, and the latter variant is predominant in meningeal SFTs. SFTs developing in the salivary glands are rare, and more rarely, those involving ectopic salivary glands (ESGs) have been reported in the cerebellopontine angle (CPA); however, their characteristics remain not well understood. In this study, we performed a clinicopathological and molecular analysis of 3 cases of meningeal SFT with ESGs. All cases presented with an extra-axial mass in the CPA, which is a rarer location for intracranial ESGs compared to the sellar region. Histologically, except for the presence of ESGs, there was no significant difference between current cases and ordinary SFTs. The ESGs demonstrated no cellular atypia, and although the spindle tumor cells were immunopositive for STAT6, the ESGs were negative in all cases, supporting that the ESGs are non-neoplastic components. In 1 case, ESGs were found only in the primary tumor and disappeared in recurrence/dissemination. Of note, molecular analysis identified *NAB2* exon 4-*STAT6* exon 2 in all cases. In conclusion, our results suggest that ESGs particularly in the CPA may be associated with SFTs and that meningeal SFTs with ESGs may be associated with the minor fusion variant of *NAB2-STAT6* in the intracranial lesions.

Keywords Solitary fibrous tumor · Hemangiopericytoma · *NAB2* · *STAT6* · Ectopic salivary gland

✉ Sumihito Nobusawa
nobusawa0319@gunma-u.ac.jp

¹ Department of Human Pathology, Gunma University Graduate School of Medicine, 3-39-22, Showa-machi, Maebashi, Gunma 371-8511, Japan

² Department of Anatomic Pathology, Graduate School of Medical Sciences, Kyushu University, Fukuoka, Japan

³ Department of Oncology, Johns Hopkins University School of Medicine, Baltimore, MD, USA

⁴ Department of Neurosurgery, Nakamura Memorial Hospital, Sapporo, Japan

⁵ Department of Cancer Pathology, Faculty of Medicine, Hokkaido University, Sapporo, Japan

⁶ Institute for Chemical Reaction Design and Discovery (WPI-ICReDD), Hokkaido University, Sapporo, Japan

⁷ Department of Neurosurgery, Daiyukai General Hospital, Ichinomiya, Japan

⁸ Iwate Prefectural Advanced Critical Care and Emergency Center, Iwate Medical University, Yahaba, Japan

⁹ Department of Neurosurgery, Japanese Red Cross Morioka Hospital, Morioka, Japan

¹⁰ Department of Pathology, Japanese Red Cross Morioka Hospital, Morioka, Japan

¹¹ Department of Radiology, School of Medicine, International University of Health and Welfare, Narita, Japan

¹² Department of Pathology, Public Tomioka General Hospital, Tomioka, Japan

Introduction

Solitary fibrous tumors (SFTs) are rare mesenchymal tumors that can occur at any location [1–4]. In the 2021 World Health Organization (WHO) classification of tumors of the central nervous system (CNS), SFTs are graded from 1 to 3 according to mitotic activity and tumoural necrosis [5]. SFTs with < 2.5 mitoses/mm² (< 5 mitoses/10 high-power field [HPF]) and no necrosis were considered grade 1; SFTs with ≥ 2.5 mitoses/mm² (≥ 5 mitoses/10 HPFs) and no necrosis were considered grade 2; tumors with ≥ 2.5 mitoses/mm² (≥ 5 mitoses/10 HPFs) and necrosis were considered grade 3. Most intracranial SFTs are dura-based; thus, the skull base, parasagittal, and falx regions are common sites, whereas the cerebello-pontine angle (CPA), pineal gland, and sellar region are uncommon sites [5].

SFT and hemangiopericytoma (HPC) were initially thought to be different tumors; however, the identification of *NAB2-STAT6* in both SFT and HPC suggests that they comprise the same tumor entity [3, 6, 7]. The presence of the fusion gene results in nuclear expression of STAT6 by immunohistochemistry [6]. *NAB2-STAT6* fusion variants have been classified into two major groups based on their hypothesized functional effects: *NAB2* exon 4-*STAT6* exon 2/3 and *NAB2* exon 5/6/7-*STAT6* exon 16/17/18 [1, 5, 8]. Several studies have suggested that the fusion gene variants are associated with clinicopathological features [1, 2, 5, 7, 9]. *NAB2* exon 4-*STAT6* exon 2/3 fusion variants have been reported to be associated with pleuro-pulmonary development, lower mitotic counts, and a lower risk of adverse events [1, 2, 5, 7, 9]. On the other hand, *NAB2* exon 5/6/7-*STAT6* exon 16/17/18 fusion variants have been reported to be associated with development from the meninges/soft tissue/head and neck, higher cellularity, and recurrent tumors [1, 3, 5, 7]. In addition to the fusion gene variants, *TP53* and *TERT* promoter mutations have been found to offer clinicopathological value in SFT; aberrant p53 overexpression and/or *TP53* mutations have been demonstrated in dedifferentiated areas of SFT, and *TERT* promoter mutation has been shown to be associated with worse prognosis [4, 7, 9–13].

Salivary gland tissue outside the major and minor salivary glands is considered as ectopic salivary glands (ESGs), with frequent sites being the mandible, ear, and mylohyoid muscle [14]. Intracranial ESGs are rare and mainly found in the sellar region. Only 3 cases of salivary gland tissue presented in the CPA have been reported [15–17]. Neoplasms involving ESGs are uncommon; outside the CNS, 35 cases have been reported, and they all were salivary gland-related tumors (Table S1) [18–30].

As intracranial tumors involving ESGs, in addition to 2 salivary gland-related tumors, 2 SFTs in the CPA have been reported; however, SFT with ESGs has not been reported outside the CNS (Table S1) [15–17, 31]. Genetic analysis was not performed for the 2 reported SFT with ESGs.

In this study, we investigated a series of 3 cases of meningeal SFT with ESGs, including 1 previously reported case, for clinicopathological and molecular features.

Materials and methods

Tumor samples

Three cases were collected for this study. Case 1 was previously reported [17]. Case 2 was from the consultation files of 1 of the authors (J.H). Case 3 was from the pathology archives of the Japan Brain Tumor Reference Center. Sections for histologic and genetic analyses were prepared from formalin-fixed paraffin-embedded (FFPE) tissue specimens. This study was conducted in accordance with the ethical committees of Gunma University (HS2016-075).

Conventional histological analysis

Three micrometer thick tissue sections were cut and stained with hematoxylin and eosin. Immunohistochemical staining was performed on FFPE tissue sections. Primary antibodies directed against the following antigens were applied: CD34 (NU-4A1; 1:100; Nichirei, Tokyo, Japan), STAT6 (S-20; 1:300; Santa Cruz, Dallas, TX, USA), p53 (DO-7; 1:50; Leica Microsystems, Wetzlar, Germany), and Ki-67 (MIB-1; 1:100; Dako, Glostrup, Denmark). For coloration, a commercially available biotin-streptavidin immunoperoxidase kit (Histofine, Nichirei, Tokyo, Japan) and diaminobenzidine were employed.

Detection of *NAB2-STAT6* fusion transcripts

Reverse transcription polymerase chain reaction (RT-PCR) was performed, as previously described [32]. Briefly, total RNA was extracted from FFPE samples using TRIzol reagent (Invitrogen, Carlsbad, CA, USA) and was reverse-transcribed using Superscript III reverse transcriptase (Invitrogen) to prepare the first-strand complementary DNA. *NAB2-STAT6* fusion assays were performed using primers described previously [32]. Each PCR product (5 μ L) was loaded onto 2% agarose gel with ethidium bromide and visualized under UV illumination.

The PCR products were also evaluated by direct sequence analysis using the Big Dye Terminator method (version 1.1; Applied Biosystems, Foster City, CA, USA) to confirm the breakpoints of the fusion transcripts.

DNA extraction and direct DNA sequencing for *TP53* and *TERT* promoter mutations

Genomic DNA was extracted from the FFPE tissue sections, as previously described [33], and was amplified and sequenced using previously described primer sets [34, 35]. PCR products were analyzed by agarose gel electrophoresis, and were then sequenced on a 3130xl Genetic Analyzer (Applied Biosystems, Foster City, CA, USA) with the Big Dye Terminator v.1.1 Cycle Sequencing Kit (Applied Biosystems) following standard procedures.

Statistical analysis

Extensive review of the English-language literature was conducted to identify previously reported cases of meningeal SFTs without ESG components with known *NAB2-STAT6* fusion variants. Fisher's exact test was performed to analyze the correlation between the fusion variants and presence of ESGs.

Results

Clinical findings

Relevant clinical data are summarized in Table 1. All 3 cases were adult females (27 to 41 years old) and presented with an extra-axial mass in the CPA. Tumors were cystic in cases 1 and 2, which showed high-signal intensity on T2-weighted magnetic resonance images (Fig. 1a) with capsule and septa showing contrast enhancement (Fig. 1b). In case 3, the recurrent tumor was solid, which showed iso- to high-signal intensity on T2-weighted images (Fig. 1c) and homogeneous enhancement on gadolinium-enhanced T1-weighted images (Fig. 1d).

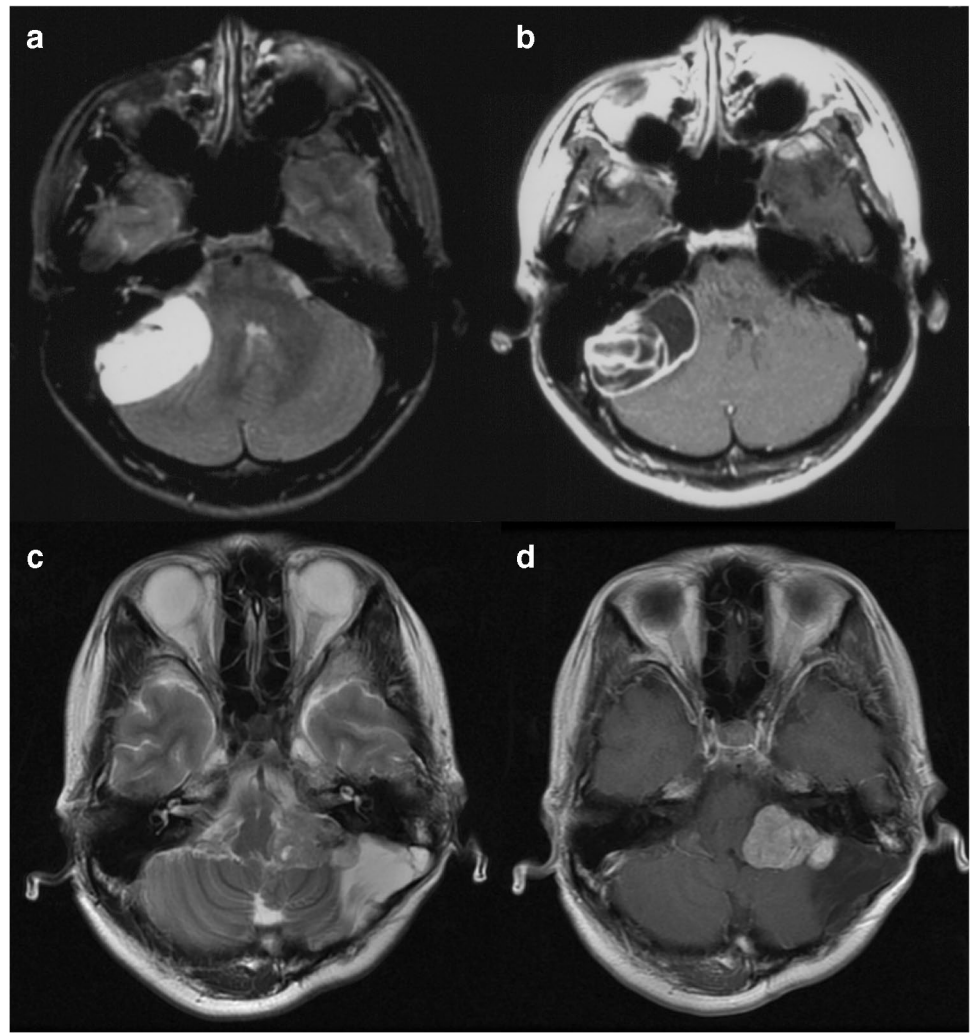
All cases underwent gross total tumor resection. In case 2, the tumor recurred locally 8 (first recurrence, R1), 18 (R2), and 19 (R3) years after the initial surgery, and excisions were performed. In case 3, although the tumor had been initially controlled by the first surgery and a gamma knife treatment at 7 years, its recurrence was more aggressive, and the patient received additional excisions at 13 (R1), 14 (R2), and 16 (R3) years after initial surgery. Multiple dissemination throughout posterior fossa and cervical spinal cord had developed at 18 years, and 2 more surgeries (R4 and R5) and 4 stereotactic radiosurgeries were performed in the next

Table 1 Case list with clinical features

Case	Age/sex	Location	Surgery	Other treatments	Recurrence, latency after surgery	Clinical outcomes
1	41/F	Left posterior fossa	Gross total resection	Preoperative embolization	No	Alive at 5 years
2	P 27/F	Right posterior fossa	Gross total resection	No	Local, 8 years	
	R1 36/F	Right posterior fossa	Gross total resection	No	Local, 10 years	
	R2 46/F	Right posterior fossa	Gross total resection	No	Local, 1 year	
	R3 47/F	Right posterior fossa	Gross total resection	No	No	Alive at 24 years
3	P 35/F	Left posterior fossa	Gross total resection	SRS (after 7 years)	Local, 6.5 years	
	R1 49/F	Left posterior fossa	Subtotal resection	No	Local, 4 months	
	R2 49/F	Left posterior fossa	Gross total resection	No	Local, 2 years	
	R3 51/F	Left posterior fossa	Gross total resection	VP shunt (after 1 month), SRS (intracranial and cervical cord, after 2 and 3 years)	Multiple (intracranial and cervical cord)	
	R4 55/F	Cervical cord	NA	SRS (multiple locations, after 2 months and 1 year)	Multiple (intracranial and cervical cord)	
	R5 57/F	Spinal cord	NA	No	Multiple (intracranial and cervical cord)	Dead, 22 years

F, female; NA, not available; P, primary; R1–R5, first-fifth recurrence, respectively; SRS, stereotactic radiosurgery; VP shunt, ventriculo-peritoneal shunt

Fig. 1 Magnetic resonance images of case 2 at initial onset (**a, b**) and case 3 at first recurrence (**c, d**). **a, b** A lobulated mass in the right cerebellopontine angle compresses right cerebellum and middle cerebellar peduncle. The mass shows very high signal intensity on T2-weighted images (**a**), suggesting a multilocular cystic mass, and the capsule and septa show contrast enhancement on gadolinium-enhanced T1-weighted images (**b**). **c, d** A lobulated mass in the left cerebellopontine angle compresses middle cerebellar peduncle. The mass shows mildly high signal intensity on T2-weighted images (**c**) and shows homogeneous enhancement on gadolinium-enhanced T1-weighted images (**d**)



4 years. The patient died 22 years after the initial surgery at her age of 57 years.

Histopathological findings

Representative histological images are shown in Fig. 2, and the histological features are summarized in Table 2. Specimens from R3 and R5 of case 3 were not available.

The lesion of case 1 demonstrated a mixture of tumor tissue and ESG components (Fig. 2a, b). The tumor was composed of spindle to ovoid cells with eosinophilic cytoplasm separated by hyalinized collagenous stroma and had variable cellularity (Fig. 2c). Necrosis and mitosis were absent, and this tumor was considered to be SFT, WHO grade 1. In addition, components of glandular structures were present in the tumor (Fig. 2a, b). The components consisted of serous and mucous acini and dilated ducts surrounded by myoepithelial cells. No cellular atypia was observed in these glandular ducts. These characteristic structures were consistent with ESGs.

The primary tumor (P) and R1–2 of case 2 showed a mixture of tumor tissue and ESG components (Fig. 2d). These tumors were focally composed of small round or short spindle cells with high cellularity with no necrosis or mitosis, and were considered to be SFT, WHO grade 1. ESGs were mixed in these tumors. Meanwhile, R3 of case 2 was composed of atypical mesenchymal cells with pleomorphic nuclei (Fig. 2e). Necrosis was absent. The mitotic rate was up to 6 per 10 high-power fields (HPFs), corresponding to SFT, WHO grade 2, and atypical mitoses were observed. These histological features were judged as dedifferentiation. ESGs remained in the tumor (Fig. 2f).

P, R1–2, and R4 of case 3 were composed of short spindle to oval shaped cells with high cellularity (Fig. 2g, h). In P and R1–2, mitotic counts ranged from 4 to 9 per 10 HPFs and necrosis was absent. These tumors were considered to be SFT, WHO grade 1 or 2. Meanwhile, brisk mitoses (21 per 10 HPFs) and necrosis were observed in R4 (Fig. 2h, i). This tumor was classified as SFT, WHO grade 3. ESGs were observed only in P (Fig. 2g).

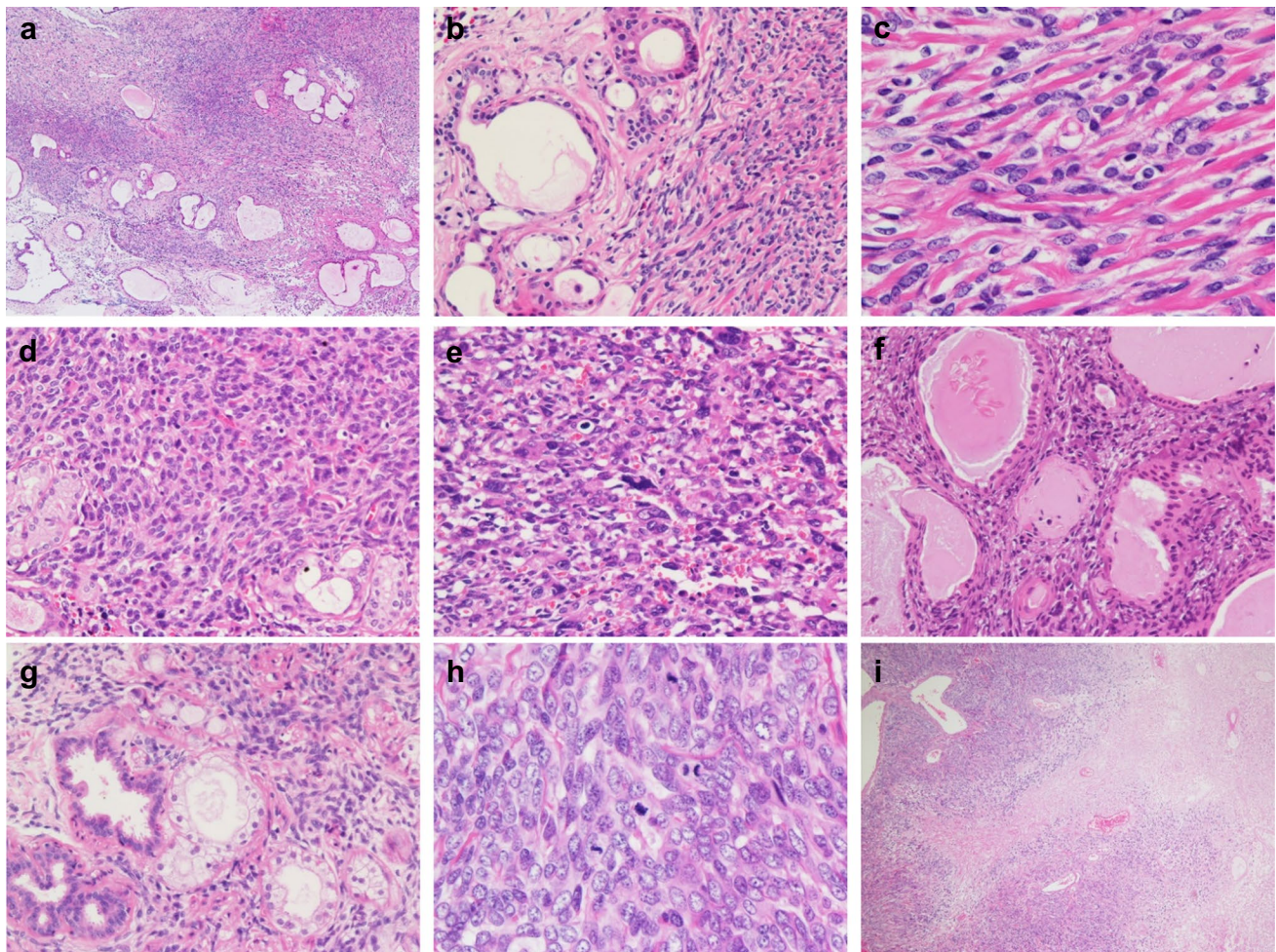


Fig. 2 Microscopic appearance. **a, b, c** The lesion of case 1 demonstrates a mixture of tumor tissue and ectopic salivary gland (ESG) components. The tumor is composed of spindle to ovoid cells with eosinophilic cytoplasm separated by hyalinized collagenous stroma. **d**, R2 of case 2 shows a proliferation of small round or short spindle cells with high cellularity. ESGs are mixed in the tumor. **e, f** R3 of

case 2 is composed of atypical mesenchymal cells with pleomorphic nuclei (**e**). ESGs remained in the tumor (**f**). **g** P of case 3 is composed of short spindle to oval shaped cells with high cellularity. ESGs are observed in the tumor. **h, i** R4 of case 3 demonstrates brisk mitoses (**h**) and necrosis (**i**). P, primary; R2–R4, second–fourth recurrence. Original magnification: **a, i** $\times 40$; **b, d, e, f, g** $\times 200$; **c, h** $\times 400$

The immunohistochemical findings are summarized in Table 2. A diffuse and strong expression of CD34 was demonstrated in case 1 and P and R1–2 of case 3. In R1 of case 2, a focal and strong expression of CD34 was demonstrated. Nuclear STAT6 positivity was observed in the spindle tumor cells but not in the ESGs in all specimens analyzed (Fig. 3a–c). The pleomorphic tumor cells in R3 of case 2 were also positive for STAT6. A diffuse and moderate expression of p53 was demonstrated only in R2 of case 2 (Fig. 3e), whereas the expression of p53 in the other specimens was negative or weakly/focally positive (Fig. 3d, f). In cases 2 and 3, the MIB-1 labeling index tended to increase along with tumor recurrence (Fig. 3g–i).

Genetic analysis

The results of genetic analysis are summarized in Table 2. RT-PCR for detecting *NAB2-STAT6* was performed for all 3 cases (for cases 2 and 3, R1 and R2 were analyzed, respectively), and they all harbored *NAB2* exon 4-*STAT6* exon 2 (Fig. 4a–c).

Direct DNA sequencing was performed for all samples available from all 3 cases except for P of case 2. Among all samples analyzed, *TP53* mutation (c.535C > T, p.H179Y) was detected only in the sample that demonstrated dedifferentiation, R3 of case 2 (Fig. 4d). No *TERT* promoter mutation was found in any samples.

Table 2 Histological, immunohistochemical, and molecular features

Case	Histology			Immunohistochemistry*1					Genetic analysis		
	Salivary glands	Mitosis (/10HPF)	Necrosis	WHO grade	CD34	STAT6	p53	MIB-1 LI (%)	<i>NAB2-STAT6</i> fusion variant	<i>TP53</i>	<i>TERTp</i>
1	+	0	-	1	3+(M/S)	+	-	7	ex 4-ex 2	-	-
2	+	0	-	1	ND	ND	ND	ND	ND	ND	ND
R1	+	0	-	1	2+(S)	+	-	1.5	ex 4-ex 2	-	-
R2	+	0	-	1	ND	+	1+(W)	2.7	ND	-	-
R3*2	+	6	-	2	ND	+	3+(M)	18.2	ND	c.535C>T p.H179Y	-
3*3	+	5	-	2	3+(S)	+	1+(W)	2.8	ND	-	-
R1	-	9	-	2	3+(S)	+	ND	26.5	ND	-	-
R2	-	4	-	1	3+(S)	+	1+(W)	19.5	ex 4-ex 2	-	-
R4	-	21	+	3	ND	ND	1+(W)	11.1	ND	-	-

*1The intensity and extent of immunopositive tumor cells were scored as follows: w, weak; m, moderate; s, strong; -, totally negative; I+, <10%; 2+, 10–50%; 3+, >50%

*2Dedifferentiated SFT

*3Specimens of R3 and R5 of case 3 were not available

*4Only exon 6 could be analyzed

P, primary; R1–R4, 1st–4th recurrence, respectively; ND, not done; ex 4-ex 2, *NAB2* exon 4-*STAT6* exon 2; *TERTp*, telomerase reverse transcriptase promoter; *MIB-1 LI*, MIB-1 labeling index; *HPF*, high-power fields

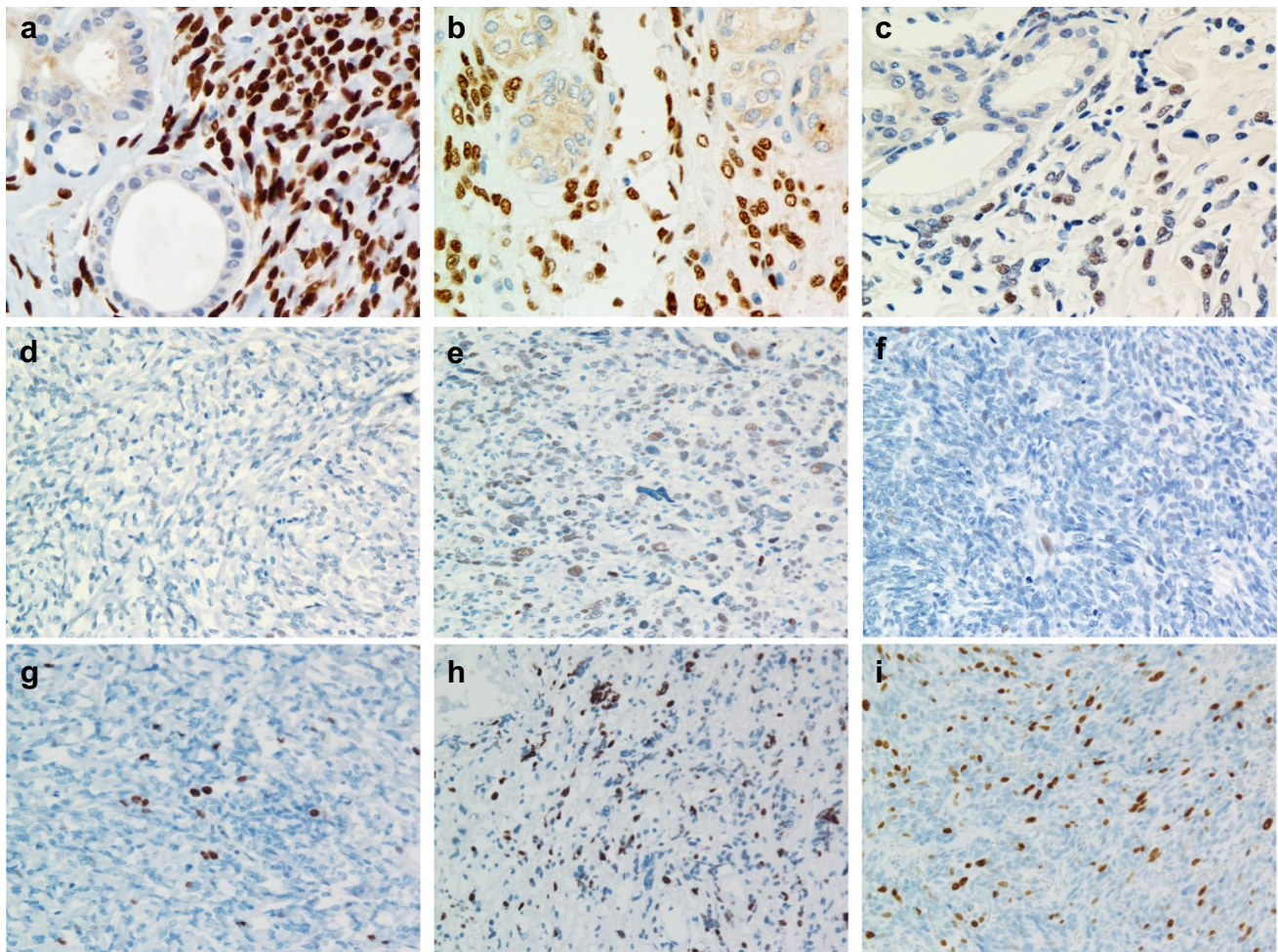


Fig. 3 Immunohistochemistry. **a, b, c** STAT6 staining. Nuclear positivity is observed in the spindle tumor cells but not in the ectopic salivary glands in all 3 cases (**a**, case 1; **b**, R1 of case 2; **c**, P of case 3). **d, e, f** p53 staining. p53 is diffusely and moderately positive in R3 of case 2 (**e**). The expression of p53 was negative in case 1 (**d**) and

focally/weakly positive in R4 of case 3 (**f**). **g, h, i** Ki-67 staining (**g**, case 1; **h**, R3 of case 2; **i**, R1 of case 3). P, primary; R1, R3, and R4, first, third, and fourth recurrence, respectively. Original magnification: **d, e, f, g, h, i** $\times 200$; **a, b, c** $\times 400$

Statistical analysis

Review of the English literature yielded 78 cases of meningeal SFTs with *NAB2* exon 4-*STAT6* exon 2/3 and 185 cases of those with *NAB2* exon 5/6/7-*STAT6* exon 16/17/18 [6–9, 13, 32, 34, 37–43]. We explored the association of *NAB2*-*STAT6* fusion variants versus the presence of ESGs, and the presence of ESGs was significantly associated with *NAB2* exon 4-*STAT6* exon 2/3 ($p=0.028$).

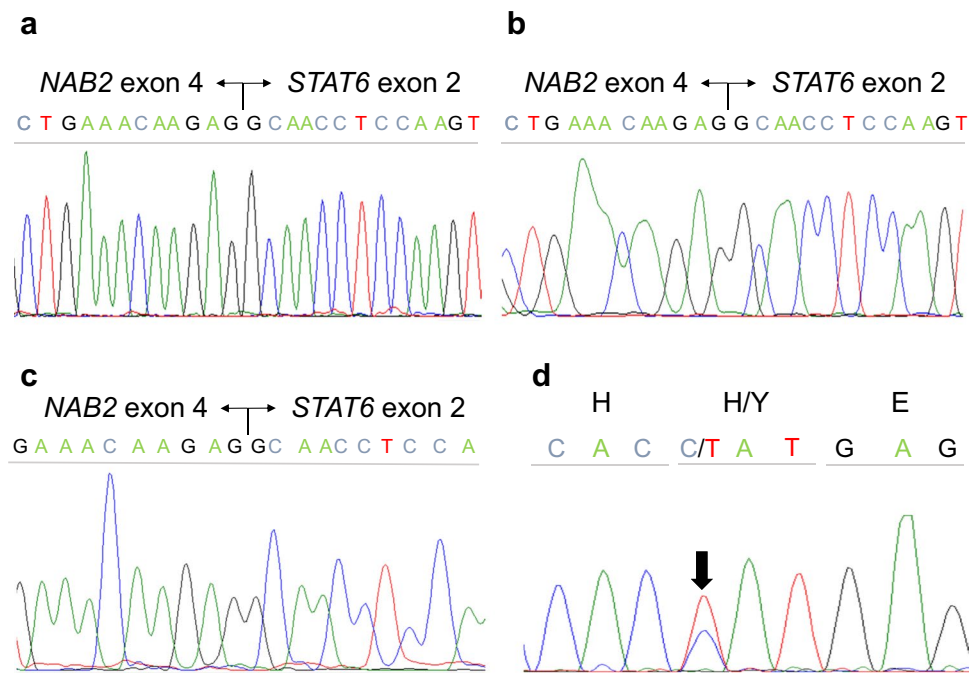
Discussion

In the present study, we described clinicopathological and molecular features of 3 meningeal SFT with ESGs in the CPA. All 3 cases harbored *NAB2* exon 4-*STAT6* exon 2, which is a minor fusion variant in meningeal SFTs.

Immunohistochemically, although the spindle tumor cells were positive for STAT6, the ESG cells were negative in all 3 cases (Fig. 3a–c), supporting that the ESG cells were non-neoplastic components. That is also in line with the findings that the ESG cells demonstrated no cellular atypia and disappeared in the specimens of recurrence/dissemination of case 3. The histologies of our cases were similar to those of reported SFTs involving non-neoplastic epithelial components other than ESGs, such as eccrine glands, orthotopic minor salivary glands, kidney, Mullerian epithelium in the omentum, and prostate [44–46]. As discussed in the previous report of case 1, due to the lack of cellular atypia in the ESG cells, carcinosarcomas as a whole or carcinomas metastasizing in SFTs were not considered [17].

Although the number of cases investigated was small, the current study showed that the presence of ESGs was associated with *NAB2* exon 4-*STAT6* exon 2 in meningeal

Fig. 4 Results of genetic analysis. **a, b, c** *NAB2* exon 4–*STAT6* exon 2 fusion was identified in all 3 cases (**a**, case 1; **b**, R1 of case 2; **c**, R2 of case 3). **d** *TP53* mutation was detected only in R3 of case 2 (c.535C>T, H179Y)



SFTs. This may reflect a difference in pathogenesis between ordinary meningeal SFTs and those with ESGs. In addition, SFTs developing in the orthotopic salivary glands are rare and 4 cases have been tested for *NAB2-STAT6* fusion variants: 2 cases with *NAB2* exon 6–*STAT6* exon 16 and 2 cases with *NAB2* exon 3–*STAT6* exon 19, with the latter being a rare variant [1, 43, 47–49]. Therefore, SFTs in the orthotopic salivary glands and those with ESGs may show different distributions of *NAB2-STAT6* fusion variants.

In case 3, ESG components were found only in the primary tumor (P) and disappeared in the recurrent and disseminated tumors (R1, R2, and R4) (Table 2, Fig. 2 g–i). Considering this phenomenon, some of the meningeal SFTs with ESGs may have been diagnosed as ordinary SFTs without ESGs, as the salivary gland components disappeared like case 3 in the current study, probably because of the overrunning of ESGs by the growth of SFTs. Sampling errors, unawareness, and underestimation may also mislead the diagnosis.

We understand that the presence of ESGs contributes to the tumorigenesis of salivary gland-related tumors, such as Warthin's tumor, pleomorphic adenoma, and mucoepidermal carcinoma; however, it is unknown whether the same is true for SFTs or whether they are only involved in the growth of tumors. If the former is true, we would expect to find SFT with ESGs in the sellar region or extracranial sites, which are more common for ESGs than CPA as mentioned before; however, there have so far not been any reports of this. Asayama et al.'s hypothesis about the developmental mechanism of SFTs with ESGs was that some salivary gland primordial cells are misplaced into dura mater during embryonic

migration and then neoplastic transformation into SFTs is brought about by the result of differentiation [17]. Along with this theory, we speculated that ESGs particularly (or only) in the CPA, as well as orthotopic salivary glands, may possess precursor cells that give rise to SFT.

On the other hand, ESGs found in 3 cases of SFTs in the current study may be the pre-existing tissue that was only embedded in the growth of tumors. If so, the absence of reports of SFT with ESGs in the sellar region, except for those in extracranial sites, does not contradict the higher incidence of conventional SFTs in the CPA than in the sellar region [50, 51]. As for meningiomas, it is now widely accepted that differences in genetic mutations (*NF2*, *KLF4/TRAF7*, *AKT1/TRAF7*, *SMO*) are associated with tumor location [52, 53]. Between *NAB2* exon 4–*STAT6* exon 2/3 and *NAB2* exon 5/6/7–*STAT6* exon 16/17/18, functional differences associated with the presence or absence of CHD4-interacting domain in *NAB2* which regulates activity of ERG1, an important regulator of fibrosis, were suggested [1]. Similar to meningiomas, it may be of interest to see whether the fusion gene variants of *NAB2-STAT6* are associated with the location of meningeal SFTs, and whether those in the CPA predominantly have *NAB2* exon 4–*STAT6* exon 2/3 fusion. However, most of the literature of meningeal SFTs that analyzed *NAB2-STAT6* variants did not describe the detailed site of lesion [6–9, 32, 37–39]; thus, further studies are needed to investigate this.

In conclusion, we report 3 meningeal SFT with ESGs harboring *NAB2* exon 4–*STAT6* exon 2 in the CPA; however, the etiological association between SFTs and the ESGs, the reason why ESGs only in the CPA have been found to

be associated with the development of SFTs, and the association between the variant of *NAB2* exon 4-*STAT6* exon 2 fusion and SFT with ESGs remain to be elucidated. Further clinicopathological and genetic analyses on more cases are needed to clarify these issues.

Supplementary Information The online version contains supplementary material available at <https://doi.org/10.1007/s00428-022-03403-7>.

Acknowledgements We thank Ms. Machiko Yokota and Mr. Tatsuya Yamazaki (Gunma University) for their technical assistance.

Author contribution S. Nobusawa designed the study; T.S., Y.Y., N.M., J.H., and S. Nobusawa performed the pathological analysis; T.S., Y.Y., Y.O., and S. Nobusawa performed the laboratory research; cases and clinical data were provided by B.A., Y.S., S.T., T.K., N. Komoribayashi, and N. Kubo; T.S., S. Nakata, N.O., and S. Nobusawa analyzed and interpreted the data; T.S., S. Nakata, and S. Nobusawa wrote the manuscript; J.H. and H.Y. participated in construction of the manuscript and revised it critically; and all authors accepted the final version of the manuscript.

Data availability Derived data supporting the findings of this study are available from the corresponding author on request.

The present study was approved by the Gunma University Ethical Committee.

Declarations

The present study was approved by the Gunma University Ethical Committee.

Conflict of interest The authors declare no competing interests.

References

- Barthelmeß S, Geddert H, Boltze C, Moskalev EA, Bieg M, Sirbu H, Brors B, Wiemann S, Hartmann A, Agaimy A, Haller F (2014) Solitary fibrous tumors/hemangiopericytomas with different variants of the *NAB2-STAT6* gene fusion are characterized by specific histomorphology and distinct clinicopathological features. *Am J Pathol* 184:1209–1218. <https://doi.org/10.1016/j.ajpath.2013.12.016>
- Tai HC, Chuang IC, Chen TC, Li CF, Huang SC, Kao YC, Lin PC, Tsai JW, Lan J, Yu SC, Yen SL, Jung SM, Liao KC, Fang FM, Huang HY (2015) *NAB2-STAT6* fusion types account for clinicopathological variations in solitary fibrous tumors. *Mod Pathol* 28:1324–1335. <https://doi.org/10.1038/modpathol.2015.90>
- Nakada S, Minato H, Nojima T (2016) Clinicopathological differences between variants of the *NAB2-STAT6* fusion gene in solitary fibrous tumors of the meninges and extra-central nervous system. *Brain Tumor Pathol* 33:169–174. <https://doi.org/10.1007/s10014-016-0264-6>
- Machado I, Morales GN, Cruz J, Lavernia J, Giner F, Navarro S, Ferrandez A, Llombart-Bosch A (2020) Solitary fibrous tumor: a case series identifying pathological adverse factors-implications for risk stratification and classification. *Virchows Arch* 476:597–607. <https://doi.org/10.1007/s00428-019-02660-3>
- Giannini C, Bouvier C, Demicco EG, Figarella-Branger D, Fritchie KJ, Macagno N, Perry A (2021) Solitary fibrous tumor. In: WHO classification of tumours editorial board (ed) WHO classification of the central nervous system tumours, 5th edn. International Agency for Research on Cancer, Lyon, pp 301–305
- Fritchie KJ, Jin L, Rubin BP, Burger PC, Jenkins SM, Barthelmeß S, Moskalev EA, Haller F, Oliveira AM, Giannini C (2016) *NAB2-STAT6* gene fusion in meningeal hemangiopericytoma and solitary fibrous tumor. *J Neuropathol Exp Neurol* 75:263–271. <https://doi.org/10.1093/jnen/nlv026>
- Park HK, Yu DB, Sung M, Oh E, Kim M, Song JY, Lee MS, Jung K, Noh KW, An S, Song K, Nam DH, Kim YJ, Choi YL (2019) Molecular changes in solitary fibrous tumor progression. *J Mol Med* 97:1413–1425. <https://doi.org/10.1007/s00109-019-01815-8>
- Vogels R, Macagno N, Griewank K, Groenen P, Verdijk M, Fonville J, Kusters B; French CNS SFT/HPC Consortium; Dutch CNS SFT/HPC Consortium, Figarella-Branger D, Wesseling P, Bouvier C, Flucke U (2019) Prognostic significance of *NAB2-STAT6* fusion variants and *TERT* promoter mutations in solitary fibrous tumors/hemangiopericytomas of the CNS: not (yet) clear. *Acta Neuropathol* 137:679–682. <https://doi.org/10.1007/s00401-019-01968-3>
- Akaike K, Kurisaki-Arakawa A, Hara K, Suehara Y, Takagi T, Mitani K, Kaneko K, Yao T, Saito T (2015) Distinct clinicopathological features of *NAB2-STAT6* fusion gene variants in solitary fibrous tumor with emphasis on the acquisition of highly malignant potential. *Hum Pathol* 46:347–356. <https://doi.org/10.1016/j.humpath.2014.11.018>
- Schiroli L, Lantuejoul S, Cavazza A, Murer B, Brichon PY, Migaldi M, Sartori G, Sgambato A, Rossi G (2008) Pleuro-pulmonary solitary fibrous tumors: a clinicopathologic, immunohistochemical, and molecular study of 88 cases confirming the prognostic value of de Perrot staging system and p53 expression, and evaluating the role of c-kit, BRAF, PDGFRs (alpha/beta), c-met, and EGFR. *Am J Surg Pathol* 32:1627–1642. <https://doi.org/10.1097/PAS.0b013e31817a8a89>
- Demicco EG, Wani K, Ingram D, Wagner M, Maki RG, Rizzo A, Meeker A, Lazar AJ, Wang WL (2018) *TERT* promoter mutations in solitary fibrous tumour. *Histopathology* 73:843–851. <https://doi.org/10.1111/his.13703>
- Bahrami A, Lee S, Schaefer IM, Boland JM, Patton KT, Pounds S, Fletcher CD (2016) *TERT* promoter mutations and prognosis in solitary fibrous tumor. *Mod Pathol* 29:1511–1522. <https://doi.org/10.1038/modpathol.2016.126>
- Maekawa A, Kohashi K, Yamada Y, Nakamizo A, Yoshimoto K, Mizoguchi M, Iwaki T, Oda Y (2015) A case of intracranial solitary fibrous tumor/hemangiopericytoma with dedifferentiated component. *Neuropathology* 35:260–265. <https://doi.org/10.1111/neup.12181>
- Martinez-Madrigal F (2019) Major salivary glands. In: Mills SE (ed) *Histology for pathologists*, 5th edn. Lippincott Williams & Wilkins, Philadelphia, pp 440–466
- Curry B, Taylor CW, Fisher AW (1982) Salivary gland heterotopia: a unique cerebellopontine angle tumor. *Arch Pathol Lab Med* 106:35–38
- Rodriguez F, Scheithauer BW, Ockner DM, Giannini C (2004) Solitary fibrous tumor of the cerebellopontine angle with salivary gland heterotopia: a unique presentation. *Am J Surg Pathol* 28:139–142. <https://doi.org/10.1097/0000478-200401000-00017>
- Asayama B, Seo Y, Ozaki Y, Tanikawa S, Hirose T, Tanaka S, Nakamura H (2019) A 41 year-old woman with a mass in the posterior cranial fossa. *Brain Pathol* 29:699–700. <https://doi.org/10.1111/bpa.12771>
- Perzin KH, Livolsi VA (1980) Acinic cell carcinoma arising in ectopic salivary gland tissue. *Cancer* 45:967–972. [https://doi.org/10.1002/1097-0142\(19800301\)45:5%3c967::AID-CNCR2820450522%3e3.0.CO;2-A](https://doi.org/10.1002/1097-0142(19800301)45:5%3c967::AID-CNCR2820450522%3e3.0.CO;2-A)
- Marucci DD, Lawson K, Harper J, Sebire NJ, Dunaway DJ (2009) Sialoblastoma arising in ectopic salivary gland tissue.

- J Plast Reconstr Aesthet Surg 62:241–246. <https://doi.org/10.1016/j.bjps.2007.09.047>
20. Wilson DF, MacEntee MI (1974) Papillary cystadenoma of ectopic minor salivary gland origin. *Oral Surg Oral Med Oral Pathol* 37:915–918. [https://doi.org/10.1016/0030-4220\(74\)90444-7](https://doi.org/10.1016/0030-4220(74)90444-7)
 21. Smith A, Winkler B, Perzin KH, Wazen J, Blitzeit A (1985) Mucoepidermoid carcinoma arising in an intraparotid lymph node. *Cancer* 55:400–403. [https://doi.org/10.1002/1097-0142\(19850115\)55:2%3c400::aid-cnrcr2820550218%3e3.0.co;2-4](https://doi.org/10.1002/1097-0142(19850115)55:2%3c400::aid-cnrcr2820550218%3e3.0.co;2-4)
 22. İsmi O, Vayisoğlu Y, Arpacı RB, Eti C, Pütürgeli T, Gorur K, Özcan C (2015) Carcinoma ex pleomorphic adenoma originating from ectopic salivary gland in the neck region: case report. *Gland Surg* 4:567–571. <https://doi.org/10.3978/j.issn.2227-684X.2015.01.03>
 23. Luksić I, Suton P, Manojlović S, Macan D, Dediol E (2008) Pleomorphic adenoma in ectopic salivary tissue of the neck. *OTO Open* 2:13–15
 24. Al-Sukhun J, Lindqvist C, Hietanen J, Leivo I, Penttilä H (2006) Central adenoid cystic carcinoma of the mandible: case report and literature review of 16 cases. *Oral Surg Oral Med Oral Pathol Oral Radiol Endod* 101:304–308. <https://doi.org/10.1016/j.tripleo.2005.06.029>
 25. Faras F, Abo-Alhassan F, Bastaki J, Al-Sihan MK (2015) Primary mucoepidermoid carcinoma arising from ectopic salivary tissue within an intraparotid lymph node. *Case Rep Otolaryngol* 2015:1–3. <https://doi.org/10.1155/2015/879137>
 26. Daniel E, McGuiert WF Sr (2005) Neck masses secondary to heterotopic salivary gland tissue: a 25-year experience. *Am J Otolaryngol* 26:96–100. <https://doi.org/10.1016/j.amjoto.2004.08.009>
 27. Tay HL, Howitt RJ (1995) Heterotopic pleomorphic adenoma in the neck. *J Laryngol Otol* 109:445–448. <https://doi.org/10.1017/s0022215100130403>
 28. Badia L, Weir JN, Robinson AC (1996) Heterotopic pleomorphic adenoma of the external nose. *J Laryngol Otol* 110:376–378. <https://doi.org/10.1017/s0022215100133675>
 29. Hata T, Iga H, Imai S, Hirokawa M (1997) Heterotopic salivary gland adenocarcinoma in the cervical region. *Int J Oral Maxillofac Surg* 26:290–292. [https://doi.org/10.1016/s0901-5027\(97\)80872-7](https://doi.org/10.1016/s0901-5027(97)80872-7)
 30. Ludmer B, Joachims HZ, Ben-Arie J, Eliachar I (1981) Adenocarcinoma in heterotopic salivary tissue. *Arch Otolaryngol* 107:547–548. <https://doi.org/10.1001/archotol.1981.00790450023007>
 31. Erdogan S, Rodriguez FJ, Scheithauer BW, Abell-Aleff PC, Rabin M (2007) Malignant myoepithelioma of cranial dura. *Am J Surg Pathol* 31:807–811. <https://doi.org/10.1097/PAS.0b013e31802c98ae>
 32. Yamada Y, Kohashi K, Kinoshita I, Yamamoto H, Iwasaki T, Yoshimoto M, Ishihara S, Toda Y, Itou Y, Koga Y, Hashisako M, Nozaki Y, Kiyozawa D, Kitahara D, Inoue T, Mukai M, Honda Y, Toyokawa G, Tsuchihashi K, Matsushita Y, Fushimi F, Taguchi K, Tamiya S, Oshiro Y, Furue M, Nakashima Y, Suzuki S, Iwaki T, Oda Y (2019) Clinicopathological review of solitary fibrous tumors: dedifferentiation is a major cause of patient death. *Virchows Arch* 475:467–477. <https://doi.org/10.1007/s00428-019-02622-9>
 33. Nobusawa S, Lachuer J, Wierinckx A, Kim YH, Huang J, Legras C, Kleihues P, Ohgaki H (2010) Intratumoral patterns of genomic imbalance in glioblastomas. *Brain Pathol* 20:936–944. <https://doi.org/10.1111/j.1750-3639.2010.00395.x>
 34. Watanabe K, Tachibana O, Sata K, Yonekawa Y, Kleihues P, Ohgaki H (1996) Overexpression of the EGF receptor and p53 mutations are mutually exclusive in the evolution of primary and secondary glioblastomas. *Brain Pathol* 6:217–224. <https://doi.org/10.1111/j.1750-3639.1996.tb00848.x>
 35. Gessi M, van de Nes J, Griewank K, Barresi V, Buckland ME, Kirfel J, Caltabiano R, Hammes J, Lauriola L, Pietsch T, Waha A (2014) Absence of TERT promoter mutations in primary melanocytic tumours of the central nervous system. *Neuropathol Appl Neurobiol* 40:794–797. <https://doi.org/10.1111/nan.12138>
 36. Nakada S, Minato H, Takegami T, Kurose N, Ikeda H, Kobayashi M, Sasagawa Y, Akai T, Kato T, Yamamoto N, Nojima T (2015) NAB2-STAT6 fusion gene analysis in two cases of meningeal solitary fibrous tumor/hemangiopericytoma with late distant metastases. *Brain Tumor Pathol* 32:268–274. <https://doi.org/10.1007/s10014-015-0220-x>
 37. Robinson DR, Wu YM, Kalyana-Sundaram S, Cao X, Lonigro RJ, Sung YS, Chen CL, Zhang L, Wang R, Su F, Iyer MK, Roychowdhury S, Siddiqui J, Pienta KJ, Kunju LP, Talpaz M, Mosquera JM, Singer S, Schuetze SM, Antonescu CR, Chinnaiyan AM (2013) Identification of recurrent NAB2-STAT6 gene fusions in solitary fibrous tumor by integrative sequencing. *Nat Genet* 45:180–185. <https://doi.org/10.1038/ng.2509>
 38. Yuzawa S, Nishihara H, Wang L, Tsuda M, Kimura T, Tanino M, Tanaka S (2016) Analysis of NAB2-STAT6 gene fusion in 17 cases of meningeal solitary fibrous tumor/hemangiopericytoma: review of the literature. *Am J Surg Pathol* 40:1031–1040. <https://doi.org/10.1097/PAS.0000000000000625>
 39. Fritchie K, Jensch K, Moskalev EA, Caron A, Jenkins S, Link M, Brown PD, Rodriguez FJ, Guajardo A, Brat D, Velázquez Vega JE, Perry A, Wu A, Raleigh DR, Santagata S, Louis DN, Brastianos PK, Kaplan A, Alexander BM, Rossi S, Ferrarese F, Haller F, Giannini C (2019) The impact of histopathology and NAB2-STAT6 fusion subtype in classification and grading of meningeal solitary fibrous tumor/hemangiopericytoma. *Acta Neuropathol* 137:307–319. <https://doi.org/10.1007/s00401-018-1952-6>
 40. Ishizawa K, Tsukamoto Y, Ikeda S, Suzuki T, Homma T, Mishima K, Nishikawa R, Sasaki A (2016) ‘Papillary’ solitary fibrous tumor/hemangiopericytoma with nuclear STAT6 expression and NAB2-STAT6 fusion. *Brain Tumor Pathol* 33:151–156. <https://doi.org/10.1007/s10014-015-0247-z>
 41. Matsuda K, Tsugu H, Hirata Y, Yoshioka T, Nishiyama K, Nabeshima K, Inoue T, Ikeda K (2018) A case of solitary fibrous tumor of NAB2 exon 6-STAT6 exon 17. *Jpn J Neurosurg* 27:228–234. <https://doi.org/10.7887/jcns.27.228>
 42. Yao ZG, Wu HB, Hao YH, Wang XF, Ma GZ, Li J, Li JF, Lin CH, Zhong XM, Wang Z, Wang DZ (2019) Papillary solitary fibrous tumor/hemangiopericytoma: an uncommon morphological form with NAB2-STAT6 gene fusion. *J Neuropathol Exp Neurol* 78:685–693. <https://doi.org/10.1093/jnen/nlz053>
 43. Bieg M, Moskalev EA, Will R, Hebele S, Schwarzbach M, Schmeck S, Hohenberger P, Jakob J, Kasper B, Gaiser T, Ströbel P, Wardelmann E, Kontny U, Braunschweig T, Sirbu H, Grützmann R, Meidenbauer N, Ishaque N, Eils R, Wiemann S, Hartmann A, Agaimy A, Fritchie K, Giannini C, Haller F (2021) Gene expression in solitary fibrous tumors (SFTs) correlates with anatomic localization and NAB2-STAT6 gene fusion variants. *Am J Pathol* 191:602–617. <https://doi.org/10.1016/j.ajpath.2020.12.015>
 44. Tran TAN (2020) Primary cutaneous solitary fibrous tumor with entrapped eccrine components. *J Cutan Pathol* 47:845–849. <https://doi.org/10.1111/cup.13717>
 45. Tapia JL, Goodloe S 3rd, Margaroni JE 3rd, Markiewicz MR, Aguirre A (2011) Solitary fibrous tumor with entrapment of minor salivary gland tissue: an unusual presentation that requires exclusion of pleomorphic adenoma. *Head Neck Pathol* 5:314–320. <https://doi.org/10.1007/s12105-011-0254-2>
 46. Zhao M, He H, Cao D, Fan D, Xu M, Zhang X, Ru G (2022) Solitary fibrous tumor with extensive epithelial inclusions. *Am J Clin Pathol* 158:35–46. <https://doi.org/10.1093/ajcp/aqab211>
 47. Rais M, Kessab A, Sayad Z, El Mourabit S, Zrarqi R, Benazzou S, Boulaadas M, Cherradi N (2017) Solitary fibrous tumor occurring

- in the parotid gland: a case report. *BMC Clin Pathol* 17:22. <https://doi.org/10.1186/s12907-017-0062-z>
48. Lee CK, Liu KL, Huang SK (2019) A dedifferentiated solitary fibrous tumor of the parotid gland: a case report with cytopathologic findings and review of the literature. *Diagn Pathol* 14:20. <https://doi.org/10.1186/s13000-019-0792-6>
 49. Gonzalez MF, Husain BH (2021) Solitary fibrous tumour of the submandibular gland: Novel insights from clinical practice on a close mimicker of pleomorphic adenoma and a diagnostic challenge for the cytopathologist. *Cytopathology* 32:261–265. <https://doi.org/10.1111/cyt.12932>
 50. Ghanchi H, Patchana T, Christian E, Li C, Calayag M (2020) Pediatric sellar solitary fibrous tumor/ hemangiopericytoma: a rare case report and review of the literature. *Surg Neurol Int* 11:238. https://doi.org/10.25259/SNI_234_2020
 51. Oishi M, Fujisawa H, Tsuchiya K, Nakajima Y (2020) The importance of STAT6 in a schwannoma-like grade III solitary fibrous tumor/hemangiopericytoma located in the cerebellopontine angle and Meckel's cave. *World Neurosurg* 141:500–506. <https://doi.org/10.1016/j.wneu.2020.05.262>
 52. Clark VE, Erson-Omay EZ, Serin A, Yin J, Cotney J, Ozduman K, Avşar T, Li J, Murray PB, Henegariu O, Yilmaz S, Günel JM, Carrión-Grant G, Yilmaz B, Grady C, Tanrikulu B, Bakircioğlu M, Kaymakçalan H, Caglayan AO, Sencar L, Ceyhun E, Atik AF, Bayri Y, Bai H, Kolb LE, Hebert RM, Omay SB, Mishra-Gorur K, Choi M, Overton JD, Holland EC, Mane S, State MW, Bilgüvar K, Baehring JM, Gutin PH, Piepmeier JM, Vortmeyer A, Brennan CW, Pamir MN, Kiliç T, Lifton RP, Noonan JP, Yasuno K, Günel M (2013) Genomic analysis of non-NF2 meningiomas reveals mutations in TRAF7, KLF4, AKT1, and SMO. *Science* 339:1077–1080. <https://doi.org/10.1126/science.1233009>
 53. Yuzawa S, Nishihara H, Tanaka S (2016) Genetic landscape of meningioma. *Brain Tumor Pathol* 33:237–247. <https://doi.org/10.1007/s10014-016-0271>

Publisher's note Springer Nature remains neutral with regard to jurisdictional claims in published maps and institutional affiliations.

Springer Nature or its licensor holds exclusive rights to this article under a publishing agreement with the author(s) or other rightsholder(s); author self-archiving of the accepted manuscript version of this article is solely governed by the terms of such publishing agreement and applicable law.